

## 2.1 Structures, properties, and nanofabrications of CNTs

### 2.1.1 Structures and properties of CNTs

Since discovery of CNTs in 1991, many superior properties of CNTs have attracted much attention of the scientists. The excellent properties of CNTs must be closely related to its unique structure. It was proposed that a graphene sheet of (0001) plane can be rolled to become various forms of CNTs structures: armchair, zigzag and chiral CNTs. The CNTs can be pictured as the fullerene-related structures with the end caps containing pentagon and hexagon rings. As shown in Fig.2-1<sup>[Dresselhaus, et al., 1996]</sup>, if a  $C_{60}$  structure is bisected normal to a five-fold axis, the “armchair” tubule can be formed. ‘Zigzag’ tubule is formed in the way of bisecting  $C_{60}$  structure normal to a three-fold axis. The other ways of bisecting  $C_{60}$  structure can form the chiral CNTs. The caps of  $C_{60}$ ,  $C_{70}$  and  $C_{80}$  [Fig. 2-1(a)] are corresponding to the CNTs structures in armchair, zigzag and chiral, respectively [Figs. 2-1(c)-(d)]. In mathematics, scientists proposed two vector to define CNTs<sup>[Saito-1992-2204]</sup>.

$$C_h = na_1 + ma_2 \equiv (n, m) \quad (2-1)$$

The  $C_h$  called chiral vector, and the angle between  $C_h$  and  $a_1$  is chiral angle  $\theta$ , while  $a_1$  and  $a_2$  denoted the unit vectors of graphene sheet. As shown in Fig. 2.2,

the structures of CNTs in zigzag, armchair or chiral form are classified by the  $\theta$  angle or range, i.e.  $0^\circ$ ,  $30^\circ$  or  $0^\circ < \theta < 30^\circ$ , respectively. The chiral vector is expressed as a pair of integers  $(n, m)$  for mapping planar graphene sheet. The zigzag, armchair and chiral CNTs are corresponding to the chiral vectors of  $(n, 0)$ ,  $(n, n)$  and  $(n, m)$ , respectively.

In 1992, Hamada<sup>[Hamada-1992-1579]</sup> and Saito<sup>[Saito-1992-2204]</sup> proposed theoretically that the CNTs can be a conductor or a semiconductor depending on its chirality. Their theories were proved experimentally by Wildoer<sup>[Wildoer-1998-59]</sup> and Odom<sup>[Odom-1998-62]</sup> in 1998, using STM. They indicated that the two parameters, helicity and diameter, can be adopted to distinguish the metallic from semi-conducting properties of CNTs, i.e. the differences in the band gap and the Fermi energy shift. Among them, the armchair CNTs have two integers  $n$  and  $m$  equal to each other, thus have bands that cross the Fermi level and therefore are truly metallic. The chiral and zigzag nanotubes had two possibilities: (a) If  $n-m = 3k$ , where  $k$  is a integer except zero, then it was metallic with an energy gap of about 1.7-2.0 eV; (b) If  $n-m \neq 3k$ , then it was semiconducting with an energy gap of about 0.5-0.6 eV [Fig. 2-3]. These show the nanotubes electrical properties are very sensitive to the wrapping angle and the tube diameter.

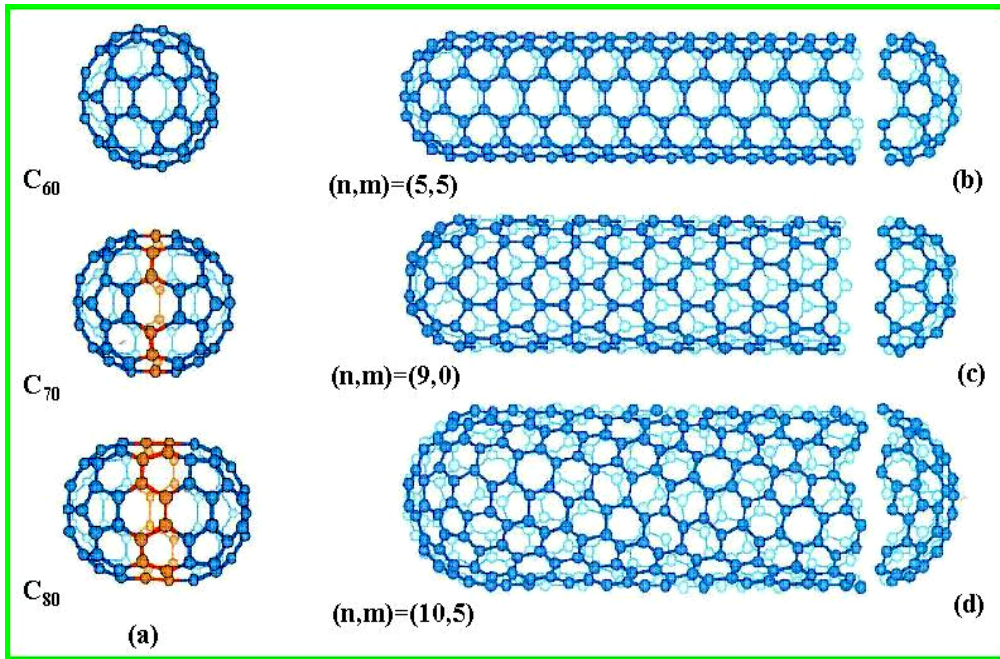


Fig. 2-1. CNT structures of armchair, chiral and zigzag tubules. [Dresselhaus, et al.,

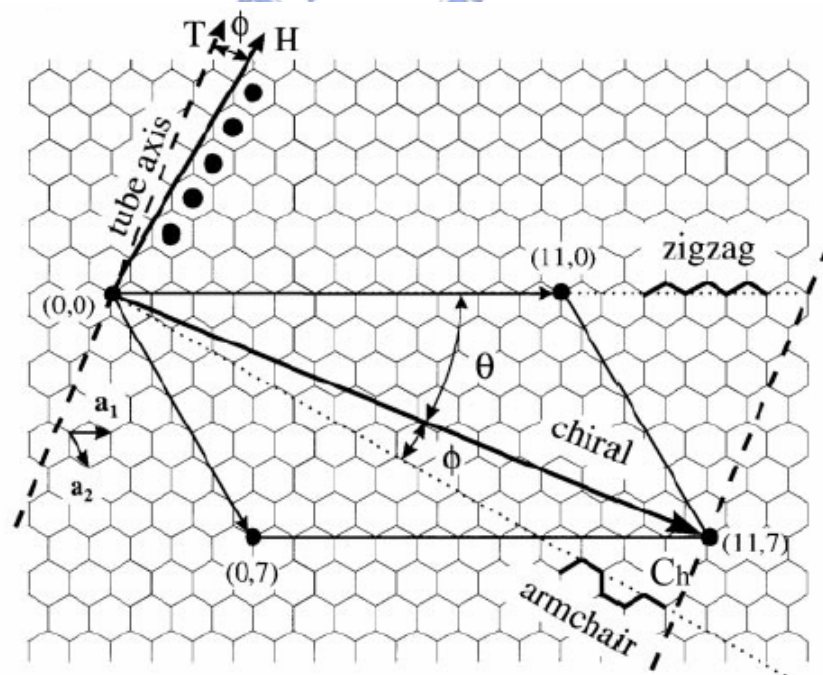
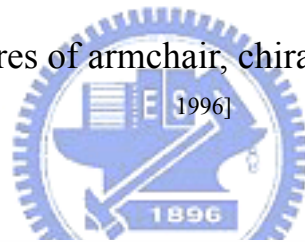


Fig. 2-2. The construction of CNT from a single graphite sheet

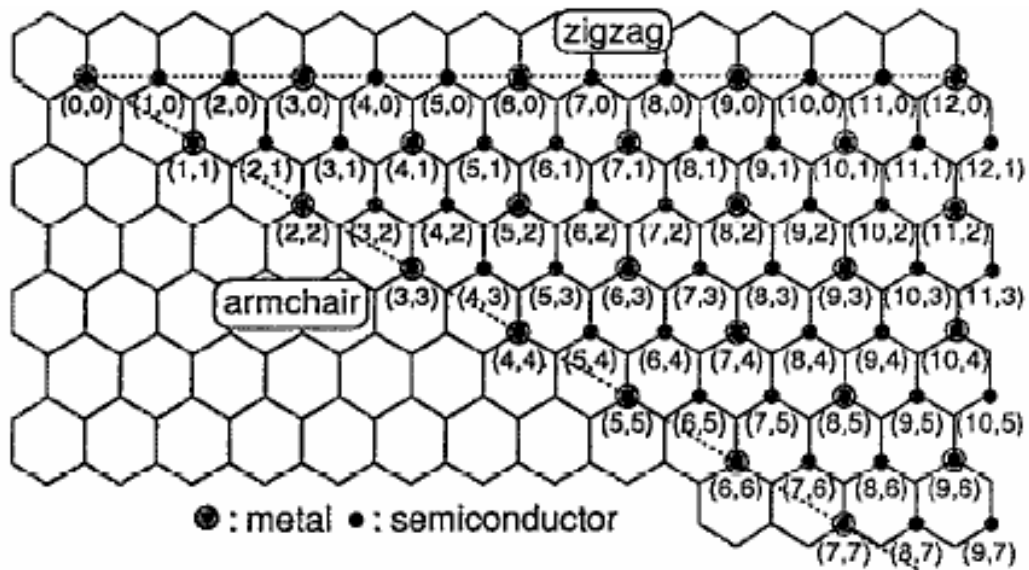


Fig. 2-3. The relation between properties and structure of CNTs

In addition to the special features on electrical properties of CNTs, another key point of what scientists concerned is their field emission properties. The field emission is an electron emission phenomenon through tunneling effect when an electric field is applied on the surface of a material with negative potential. Due to suitable geometric contours, high thermal stability, good mechanical strength and high chemical stability, CNTs becomes a good field emission material. The field emission is much more fascinating than thermal emission since it just needs to apply a low electrical field ( $\sim V/\mu\text{m}$ ) at room temperature. Usually, the field emission properties can be expressed by Fowler-Nordheim equation [Spindt, et al., 1976] :

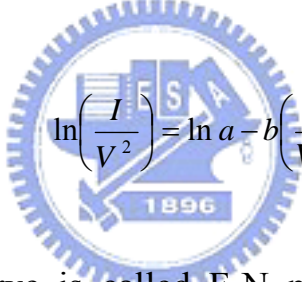
$$I = aV^2 \exp\left(\frac{-b}{V}\right) \quad (2-2)$$

$$a = \frac{\alpha A \beta^2}{1.1\phi} \exp\left[\frac{B(1.44 \times 10^{-7})}{\phi^{1/2}}\right] \quad (2-3)$$

$$b = \frac{0.95 B \phi^{3/2}}{\beta} \quad (2-4)$$

$$\text{with } A = 1.54 \times 10^{-6}, B = 6.87 \times 10^7 \quad (2-5)$$

where  $I$ ,  $V$ ,  $\phi$ ,  $\alpha$  and  $\beta$  are the field emission current (A), an applied voltage (V), a work function of material (eV), the effective emission area (m<sup>2</sup>), and the field enhancement factor, respectively. Base on Eq. 2-2, one can obtain :



$$\ln\left(\frac{I}{V^2}\right) = \ln a - b\left(\frac{1}{V}\right) \quad (2-6)$$

The  $\ln\left(\frac{1}{V^2}\right)$  versus  $\frac{1}{V}$  curve is called F-N plot. A material with good field emission properties often shows a negative slope on the F-N plot. Base on Eq. (2-2), the ways to improve the field emission properties of a material can be achieved by increasing the effective emission area,  $\alpha$ , and the field emission factor,  $\beta$ , which is related to the aspect ratio or geometric factor of emitter. Furthermore, the too-close distance between emitters can deteriorate their emission properties, which is often called the screen-effect.<sup>[Gröning-2000 -665]</sup> This signifies that the manipulation of the tube number density is also an important issue in field emission studies.

In addition to special marvelous electrical properties, the mechanical properties of CNTs are excellent, e.g. the reported Young's modulus may reach over 1 TPa <sup>[Eric-1997-1971]</sup> which makes CNTs the stiffest material in the world. CNTs also behave elongation to failure of 20-30% <sup>[Pan-1999-3152]</sup> with a high tensile strength about 60 GPa <sup>[Yu-2000-637]</sup>. These experiment values enable the CNTs to become the highest strength/weight ratio material on earth, and to be used for potential applications in reinforcement of the composites.

## 2.1.2 Nanofabrication of CNTs

There are many methods being developed to synthesize CNTs, where arc-discharge, laser ablation and chemical vapor deposition (CVD) are the most popular methods. In those methods, carbon sources can be in gas or solid phases. The morphology and properties of CNTs are often controlled by manipulating the following process parameters: substrate temperature, precursor gases and gas ratio, catalyst, pretreatment conditions, applied bias, etc. However, the proposed methods still suffer the following problems: low yielding, low uniformities in structure and property, etc.

### (a) Arc-discharge method

Arc-discharge method is believed to be the earliest way to synthesize CNTs. When CNTs were found for the first time by Iijima <sup>[Iijima-1991-56]</sup>, it was produced

by this method. Figure 2-4 shows the schematic diagram of the arc-discharge system. There are two graphitic rods as anode and cathode. Between these two electrodes, arcing occurs when DC voltage is applied. In the situation of anode containing small amount of catalyst such as Fe, Co, Ni and Y, the SWNT can be synthesized<sup>[Bethune-1993-605]</sup>, and MWNTs can be fabricated by using pure graphite as two electrodes. Generally, the discharge is operated at a voltage range between 20 and 40 V with current from 40 to 100 A under He or Ar atmosphere of 10-500 Torr. Carbon clusters collided out from the anodic graphite rod by electron bombardment are deposited on the cathode surface. The production on cathode may include amorphous carbon, fullerenes, carbon cluster, carbon nanotubes and varieties of other carbon structures. Therefore, purification of the nanostructures is generally an important issue for applications. Another drawback of this process is its low yielding in producing CNTs.

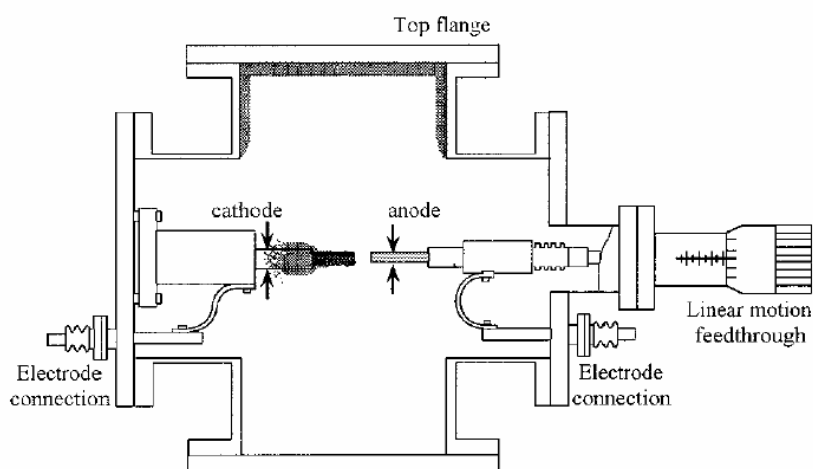


Fig. 2-4. Schematic diagram of arc-discharge system

## (b) Laser ablation

Laser ablation method was first reported by Guo's group in 1995<sup>[Guo-1995-49]</sup>, as shown schematically in Fig. 2-5. There is an incident laser beam for vaporizing graphite target under helium or argon gas atmosphere at pressure of 500 Torr. The productions are swept out by the flowing gas and to be deposited on the water cooled collector. Therefore, it is also called laser vaporization method. The graphite target containing Co, Ni, Fe, or Y is a more favor condition to form SWNTs.

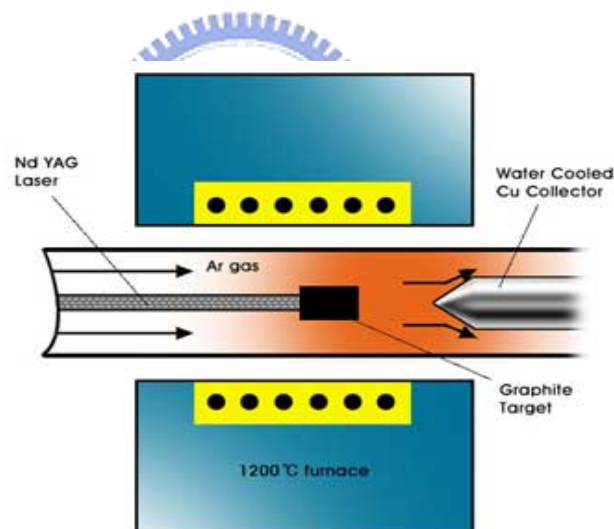


Fig. 2-5. Schematic diagram of laser ablation system

## (C) Chemical Vapor Deposition (CVD)

The CVD method is a mature technique in thin film processes. Most of films can be fabricated by CVD method, including metals, semiconductors and insulators. It is essential for CVD process to introduce some forms of the energy to decompose precursor gases and deposit the reaction product on the substrate



surface. The introduced energy may include thermal, microwave, rf, or others. Thus, it gives rise to different process names, depending on the source of the applied energy. Various CVD processes to synthesize CNTs has been proposed by many researchers, including MPECVD<sup>[Tsai-1999-3462]</sup>, ECRCVD<sup>[Lin-2002-922]</sup>, rf-PECVD<sup>[Yeon-2002-129]</sup>, thermal CVD<sup>[Lee-2000-3397]</sup> [Fig. 2-6], hot filament CVD<sup>[Tu-2002-4018]</sup>, etc. Regarding the use of CVD methods for CNTs growth, many growth mechanisms have been proposed. However, most of the mechanisms are based on the original model of carbon nanofibres proposed in 1970s by Backer.<sup>[Backer-1978-14]</sup> It is believed that nanotubes grow as carbon precipitates from a supersaturated metal catalyst that resides at either the base or the tip of a growing nanotube. Catalyst/substrate interactions and temperature gradients across the catalyst particle are considered to be important factors that determine the growth mechanism. However, most of these models were proposed without sufficient and systematic supporting experimental evidence, and they often lacked details about the physical mechanisms and the effects of various process parameters. Thus, the kinetics of nanotube nucleation and growth are not well known yet.

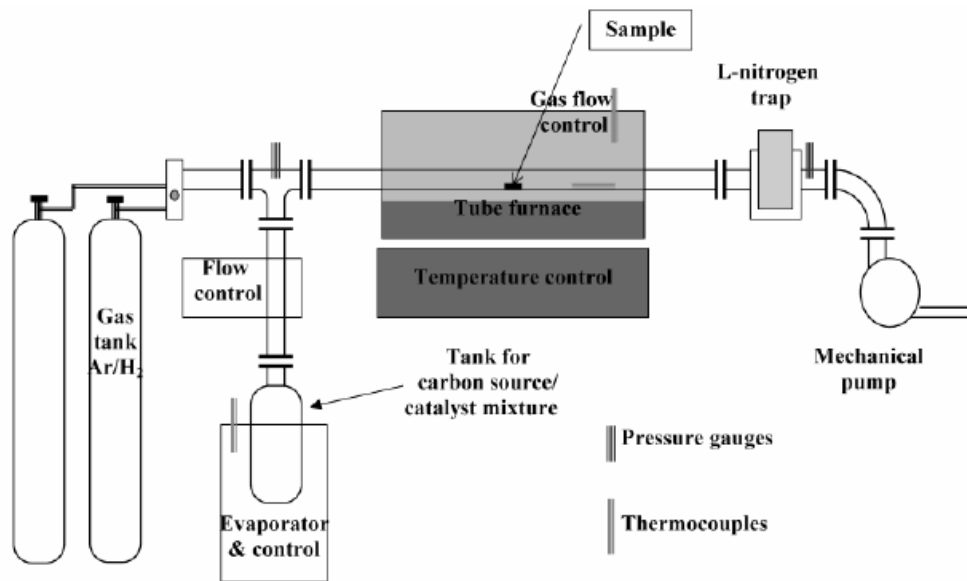


Fig. 2-6. Diagram of thermal CVD<sup>[Lee-2000-3397]</sup>

### 2.1.3 The process parameters of growth CNTs in ECR-CVD

It is well-known that the microwave plasma ECR-CVD has advantages of high dissociation percentage of precursor gases and high uniformity of plasma energy distribution.<sup>[Lin-2002-922, Sung-1999-197]</sup> It is generally used for large area dry etching, surface cleaning, or diamond film deposition. Moreover, its working pressure is lower relatively to other CVD implying cleaner deposition environment. It is very important to finely control the process condition during growth CNTs. Different parameter can result in distinct properties of CNTs e.g. morphology, growth mechanism, tube number density, structure, etc.

#### (a) Catalyst :

Different catalysts own distinct properties and the growth of CNTs can be

affected. If a catalyst particle is tightly sintered, it becomes harder to melt during reduction or pretreatment process. In other words, to form nano-scaled liquid droplets which provides the embryo of CNTs is more difficult, so the same catalyst leads to the growth of nano-sheet instead of nanotube with lower growth temperature.<sup>[Lin-2002-922]</sup> The ways of depositing catalyst also cause influences as well.

(b)Growth temperature :

Besides the above-mentioned influence of catalyst reduction, temperature can also affect the diffusion rate of carbon atoms inside the catalyst. With higher growth temperature, the diffusion rate within catalyst becomes quickly and direct affects the growth rate, length and tube number density of CNTs. Also, the precursor gases decompose amount can be different with different temperature. It changes the mixing concentrations of precursors. In addition, the crystalline of graphene layer becomes better with higher growth temperature.

(c)Gas

This condition includes precursor type and flow rate. In literature, many carbon source and reducing gas has been used.<sup>[Yun-2003-6789][Lin-2002-922]</sup> Different gas types have distinct pyrolysis temperature and different bombardment effect in plasma environment.

(d) Bias

In an ECR-CVD chamber, bias is an essential condition for well-align CNTs. During growing, CNTs will be guided by the direction of bias electrical field growing along the course.

(e) Working pressure :

When the inlet and pumped out gas flow reach a steady state, the pressure in chamber is called working pressure. The main effects of this parameter are the plasma behavior. With higher pressure, the mean free path of radical decrease but collision probability increase. The plasma induced self-bias will change with different pressure.



(f) Growth time

Growth time usually change the length of CNTs. But after catalyst is poisoned, the growth time won't affect it any more.

## 2.1.4 Application of CNTs

Many researchers and engineers have been devoted to combine the CNTs with living. There are a lot of possible applications of CNTs products such as FED, field effect transistor (FET), hydrogen storage, etc. Until now, lots of prototypes of these applications have been published. Thus, it is believed that more and more commercial products will be published soon in the future.

(a) Electron field emission elements:

The electron field emission elements, as implied by the name, utilized the field emission properties of CNTs. Among all of them, the closest to our life is FED. It is a next generation display after plasma display panel (PDP) and liquid crystal display (LCD) technologies. The theorem of formation of image is to use CNTs as cathode, then applies the potential between cathode and anode. Electrons emits from cathode to anode with phosphors which generate illumination. Ultra thin, wider view angle, superior brightness and low operation power are main advantages of FED. Samsung corporation had been public the 4.5' FED prototype in 1999 [Fig. 2-7].<sup>[Choi-1999-75-3129]</sup> And the electron source like SEM filament<sup>[Chow-1992-1]</sup> or X-ray tube<sup>[Yue-2002-355]</sup> can also employ the CNTs as electron emitters, which possess longer life, small energy spreading and power-saving significantly. Another field emission application related to general public is cathode-ray tube (CRT) lighting elements. The original has been published in 1998 by Ise Electronics corporation, Japan.<sup>[Saito-1998-L346]</sup> The fabricated CRTs are of a triode type, consisting of a cathode (nanotubes field emitter arrays), a grid and an anode (phosphor screen) [Fig.2-8(a)(b)]. The maxima brightness with anode at  $200 \mu A$  is  $64000 \text{ cd/cm}^2$ . Stable electron emission, adequate luminance and long life (over 10000 hours) are demonstrated. It can be applied to a giant outdoor display or ultra-high quality color CRT displays.

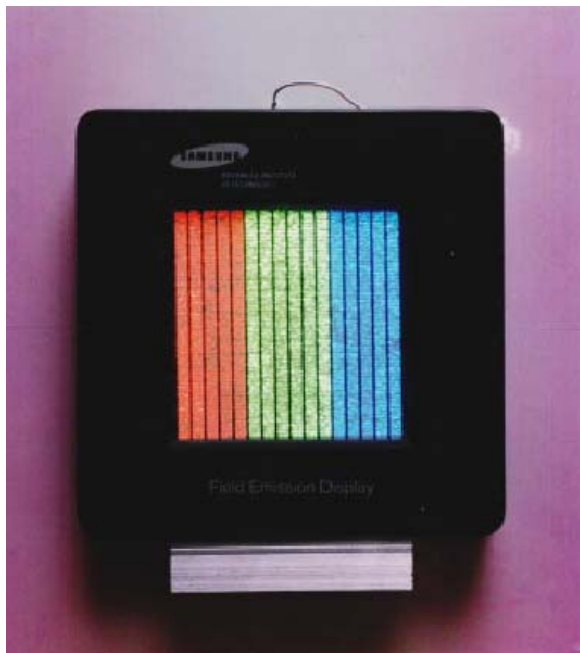


Fig. 2-7. FED display at color mode with red, green, and blue phosphor column.

[Choi-1999-75-3129]

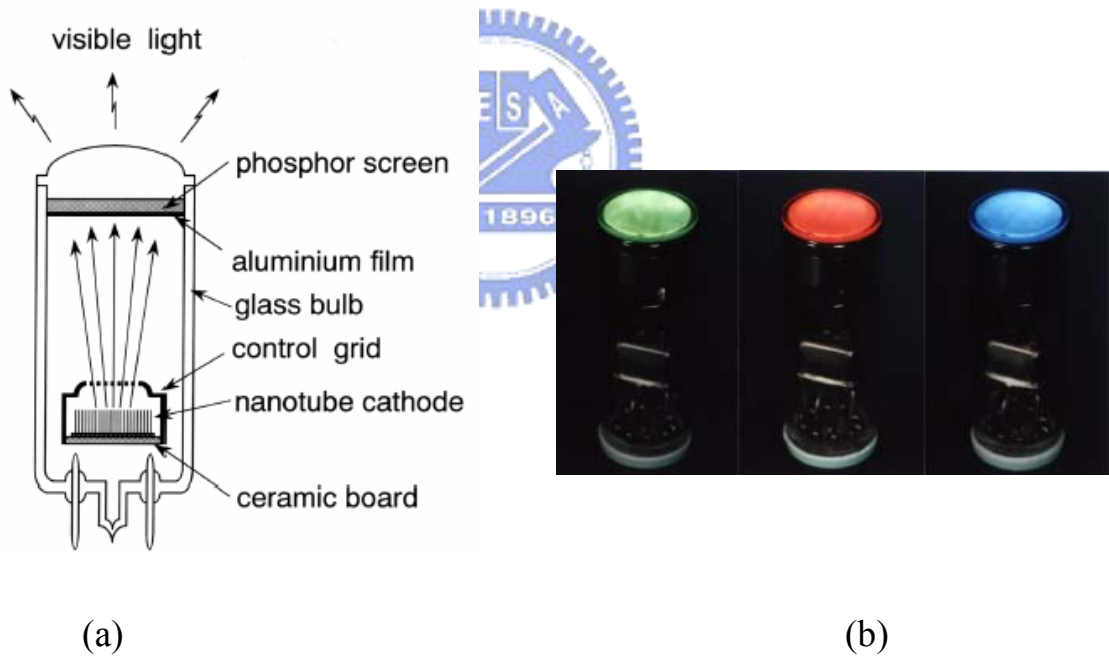


Fig. 2-8. Schematic drawing (a) and physical object (b) of a longitudinal cross section of a CRT fluorescent display with a field emission cathode composed of carbon nanotubes. [Saito-1998-L346]

(b)FET

FET is a very important electronic device in history. The overwhelming

majority of FET is silicon or III–V based just because these materials are semiconductors. But some of CNTs also have semiconducting properties, it makes researchers want to fabricate the CNTs based FET. In 1998, Sander reported the room-temperature transistor based on a single SWNTs FET.

[Sander-1998-393-49] Fig. 2-9 shows the I-V curve of the CNT-FET. In 2001, Derycke in IBM corporation prepared both p-type and n-type nanotubes transistors to build the first nanotubes-based logic gates: voltage inverters [Figs.2-10(a), (b)].

[Derckye-2001-453] Surely, it still have lots of complicated problems to mass production above-mention devices, but these results have told that the nano-electronics is not hollow words any more.

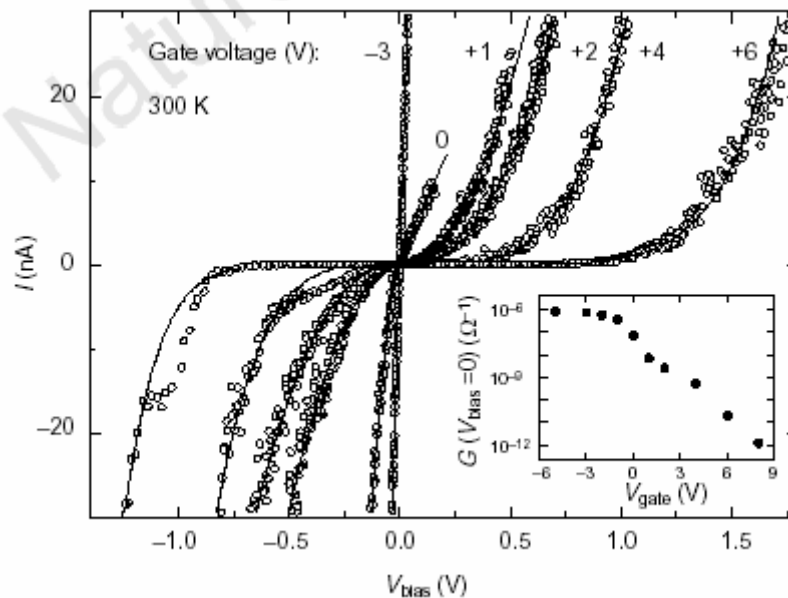


Fig. 2-9. Two probe I- $V_{\text{bias}}$  curve for various values of the gate voltage from a CNTs-based FET. [Sander-1998-393-49]

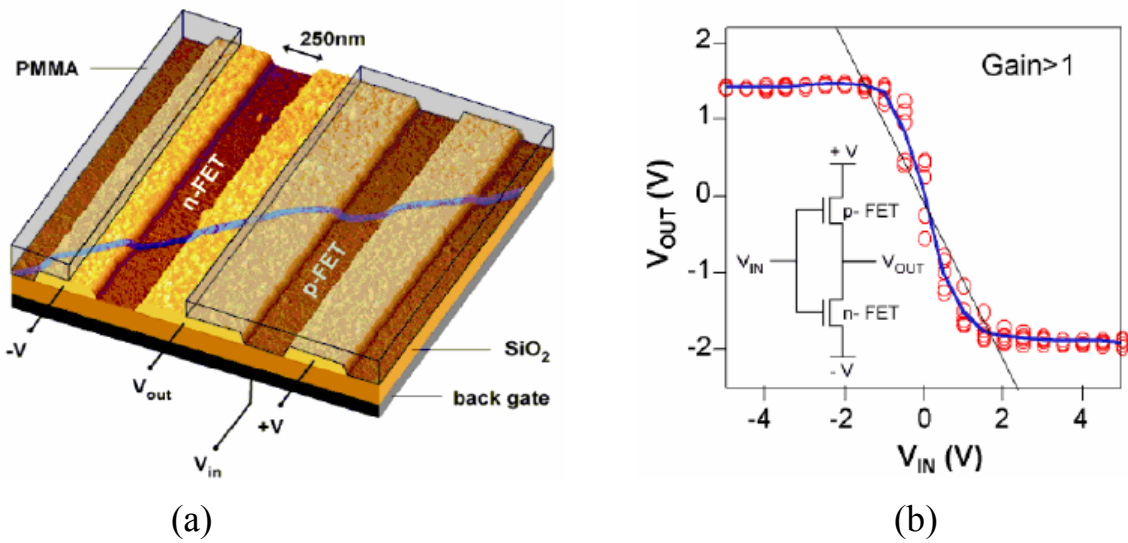


Fig. 2-10 (a) Atomic Force Microscopy (AFM) image shows the design of the voltage inverter. (b) Characteristics of the resulting intramolecular voltage inverter. [Derckye-2001-453]

### (c) Hydrogen storage material

Face to possible energy-crisis of gasoline, people has started to find the substitution methods for many years. Fuel cell was considered to have potential among all of solutions. Once it does be generated, its use as a fuel that creates neither air pollution nor greenhouse gas emissions. But it needs a huge hydrogen storage capability material. CNTs just can play this role.<sup>[Liu-1999-1127]</sup> CNTs can absorb higher hydrogen than conventional materials.<sup>[Chen-1999-91] [Liu-1999-1127]</sup> The hydrogen storage mechanisms of CNTs are still not well known yet, and these properties usually occur at high pressure or low temperature environment. It remains impossible to apply on commercial product so far.



(d) Another applications

Atomic Force Microscope (AFM) is employed to obtain the surface morphologies and roughness. It uses a probe scanning the surface of sample, and an incident laser beam irradiates the arm of probe reflecting to a detector which passes signals to computer and draws the images. In order to obtain a high resolution images, the tip must be ultra thin, extremely sharp and high strength. General type of AFM tip is made of  $\text{Si}_3\text{N}_4$ . The first article that utilized MWNTs as AFM tip was reported in 1996[Fig. 2-11].<sup>[Dai-1996-147]</sup> From Fig. 2-12, one can clearly see the CNTs tip shows the better image resolution. At the same time, CNTs with excellent mechanical properties can make the damage ratio of tip decrease as low as possible. It has been some commercial products of CNTs AFM tip at present.



In 1998, Wong demonstrated that CNTs tip can be used for chemical and biological discrimination.<sup>[Wong-1998-52]</sup> Another possible application applied to biotechnology of medicine carriers are developing as well. In the future, people will easily get to know what disease that we get. Also, people can use CNTs filled with drugs injecting into body, then induce it to the proper position relaxing the medicine to destroy the etiology without hurting normal cell nearby.

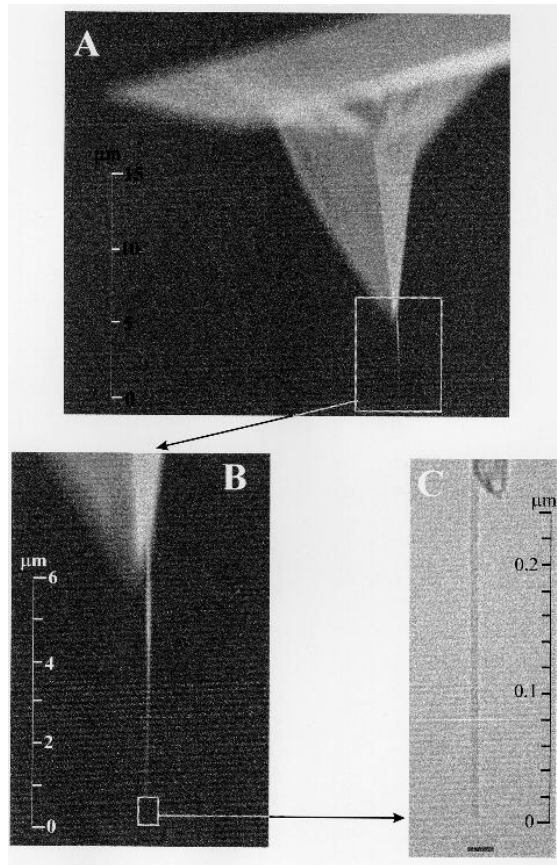
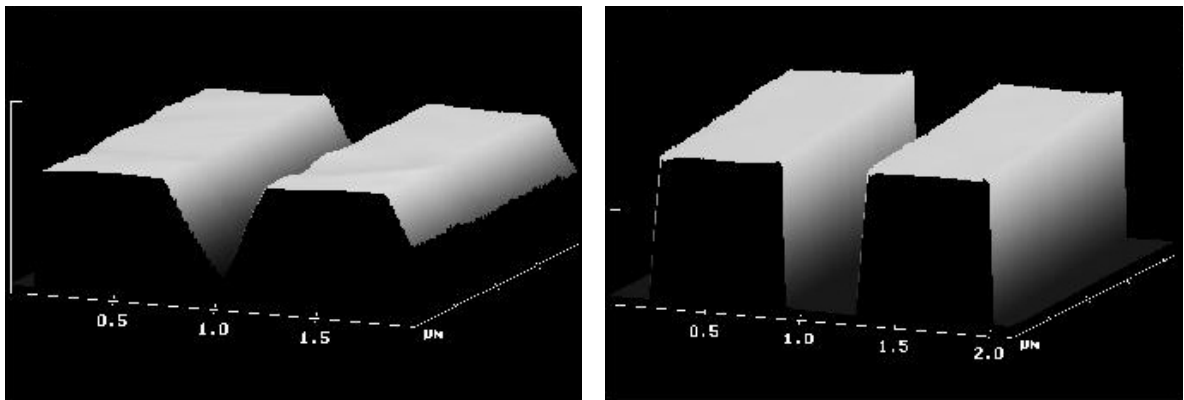


Fig. 2-11. SWNT attached to the pyramidal tip of a silicon cantilever for AFM.  
 [Dai-1996-147]



(a)

(b)

Fig. 2-12. (a) Tapping mode AFM image of a 400-nm-wide, 800-nm-deep trench taken with a bare pyramidal tip. (b) The image taken with a nanotubes attached to the pyramidal tip with the same specimen.  
 [Dai-1996-147]

## 2.2 Anodic Aluminum Oxide(AAO)

### 2.2.1 Characteristic of AAO

Nanoporous aluminum oxide forms during anodization of aluminum in acidic electrolytes [Fig. 2-13]. At first, anodization of Al surface was for protection or decoration commercially. In recent years, porous anodic alumina with an ordered nanopore array has attracted an increasing interest, because of its favorable applications as a template in fabricating nanostructure materials.

The pore structure of AAO films is a self-ordered closely packed regular array of hexagonal columnar cells. These cells contain cylindrical nanopore normal to the Al surface [Fig. 2-14]. In the figure,  $D_p$  means the pore diameter and  $D_c$  the cell distance. There is an alumina layer called barrier at the bottom of AAO as well. This layer always does exist, and this causes some problem to practice subsequent step in specific processes due to its insulation. When Al is anodized into aluminum oxide, the volume expands. The strain energy from the volume expansion at the metal/oxide interface can result in porous layer self-organizing into a two-dimensional densely packed hexagonal pore structure. <sup>[Jessensky-1998-1173, Li-1998-2470]</sup> Under controlled anodization conditions like electrolyte, concentration or anodizing voltage, ordered pore structures have been prepared by anodization in oxalic, sulfuric, and phosphoric acid solutions. <sup>[Li-1998-6023]</sup> However, the ordered pore arrangement is generally obtained only in

domains with sizes in the range of a few micrometers.<sup>[Li-1998-6023]</sup> In general, the merits and drawbacks of AAO are listed in Tab 2-1.

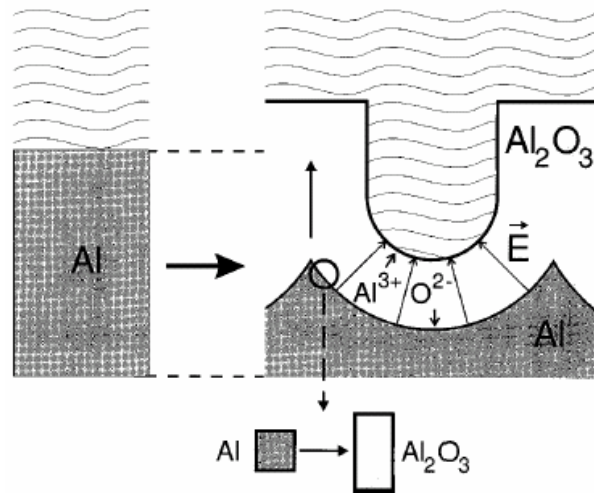


Fig. 2-13. Diagram of the ions moving directions during aluminum oxidation.

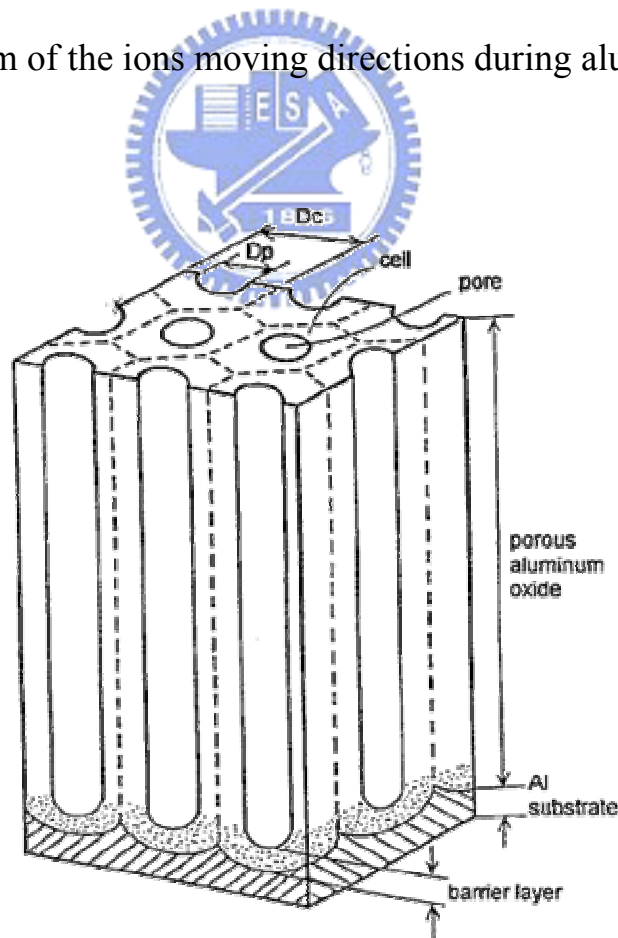


Fig. 2-14. Structure of AAO<sup>[Li-1998-2470]</sup>

Merits	Drawbacks
Easy fabrication	Short range order
High aspect ratio	
Relative order within domains	
Uniform size and length	

Table 2-1 Merits and Drawbacks of AAO

## 2.2.2 Nanofabrication of AAO

In brief, when put an aluminum metal in an acid solution, then applies anodic voltage, one can easily get an aluminum oxide layer above the surface of aluminum. This is a very simple, cheap, and cleaning-room-free fabrication process. It seems so effortless to get an AAO membrane, but is fairly complicated to get an ordered nanopore array. This situation is more apparent on a deposited aluminum film than an aluminum sheet. The dynamic of ordered AAO arrays depends on the mechanical stress at the metal/oxide interface.<sup>[Li-1998-2470]</sup>

Following the increase on anodization time, arrangement of these pores shows more and more regular. So, the simplest way to get ordered nanopore array is proceeding a long time anodization. Nevertheless, there are three big problems with long time anodization. One, the process will waste lots of time. Two, it needs aluminum thick enough for long time anodization. Three, the pore distributions of surface remain random. For the reasons, many research teams intro-

duce into so-called two step anodization process.<sup>[Masuda-1996-L126]</sup> In the method, first anodization layer is removed by wet chemical etching because it would make irregular arrangement of pore array and obtain a pre-structured Al film. Then, the second anodization is proceeded to fabricate regular arrangement nanopores. Another way to get an ordered AAO array is defining a pre-pattern Al surface by lithography or else.<sup>[Li-2000-131]</sup> When practice anodization, the pre-pattern positions own the priority to form pores. However, when the pore growth, it returns to the hexagonal morphology without affect by surface pattern.

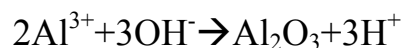
Besides, the process condition e.g. electrolyte concentration, temperature, anodic voltage, fabrication method of aluminum, etc, will affect the range of ordered area and interpore distance. The ordered pore arrays prepared in oxalic and sulfuric acids are of relative small interpore distances of 50-100 nm. Porestructures with a pitch as large as 420 and 500 nm were demonstrated by using phosphoric acid as electrolyte although the structures contained many defects.<sup>[Li-1998-6023][Masuda-1998-L1340]</sup>

### 2.2.3 Growth mechanism of Nanoporous alumina

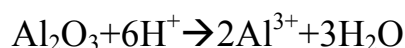
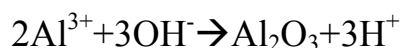
Nanoporous alumina formed by anodization has been widely studied during the last few decades. This nanoscale pattern formation phenomenon by electrochemical reactions has also attracted many theoretical studies to decipher its in-

stability mechanism and to determine the selected time and length scales, but without much success. In spite of the surfeit of experimental data, the basic mechanism behind pore formation phenomenon still awaits explanation and a self-consistent theory.

Here, the possible ways that were accepted by people widely are reported. There are two forms of AAO exist, the nonporous barrier oxide and the porous oxide. When Al is anodized in neutral or basic solution, a flat, nonporous, featureless insulating “barrier” oxide forms.<sup>[Lohrengel-1993-243]</sup> When Al is anodized in an acid, deep pores can form. Whatever the methods of fabricating Al, it is impossible for the surface of Al to reach the absolute flat state in fine view. During the initial stage of pore formation, some small pits on Al surface suffer more electric field due to the curvature itself and the ionic current density at the pore bottoms more than between the pores. Thus, the pores start growth. The electrochemical reactions and ionic paths involved during anodization of Al can represent in Fig. 2-15.<sup>[Sunil-2002-12-240]</sup> At metal/oxide interface, the reactions are:



And at the oxide/electrolyte interface, the reactions are :



The fig. 2-16 shows the characteristic current density versus time ( $j$  vs  $t$ ) for a constant voltage anodization of aluminum in an acidic electrolyte. <sup>[Sunil-2002-12-240]</sup>

In literature, Thompson, Wood, and co-workers<sup>[Thompson-1983-205]</sup> proposed that pore nucleation is due to a cracking and self-healing of the oxide layer atop preexisting ridges on the Al surface and that this forms a barrier layer of non-uniform thickness. <sup>[Shimizu-1992-643]</sup> In 1998, Li et al. designed a series of experimental<sup>[Li-1998-2470]</sup> to make a thorough inquiry how the pores form. They only changed anodic time in a short period and utilized AFM and SEM as main analytical instrument to observe surface morphology. Besides, they measured the relationship of current density( $j$ ) vs. time( $t$ ) , voltage( $V$ ) vs time( $t$ ) and regular domain size area vs. time with different anodic temperature. From the proposed literature and their observation of experimental phenomena, they concluded that the hydrogen ions and the electric field at the oxide/electrolyte interface must play important roles during nanoporous formation. And the pore nucleation occurs as the barrier layer is first formed, concentrates where the oxide is thinnest, and involves an acid-catalyzed partial oxide dissolution at the pore bottoms where the electric field is highest. In 2002, Sunil and Chang used mathematical formula and computer assisted calculation to predict the transition from porous to nonporous alumina at a  $\text{PH}=1.77$  <sup>[Sunil-2002-240]</sup>. It also proved the hydrogen ion is an essential key player in this process.



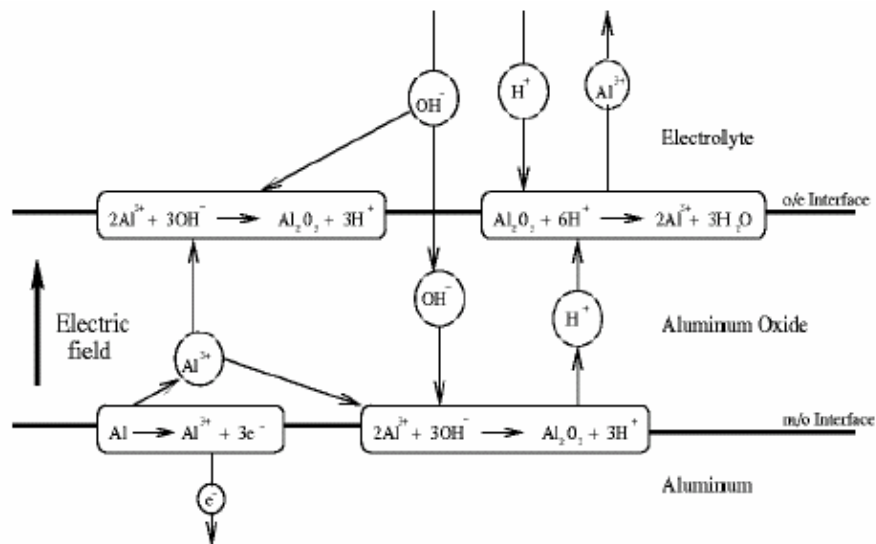


Fig. 2-15. Schematic diagram showing the electrochemical reactions and ionic paths involved during anodization of aluminum. [Sunil-2002-12-240]

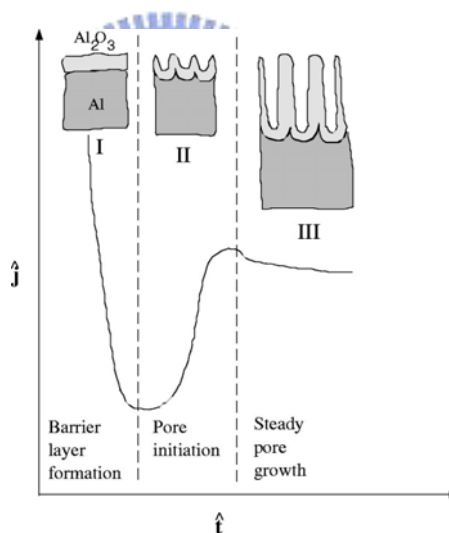


Fig. 2-16. A schematic diagram showing the characteristic current density versus time ( $\hat{j}$  vs.  $\hat{t}$ ) for a constant voltage anodization of aluminum in an acidic electrolyte. [Sunil-2002-240]

## 2.3 Growth of CNT arrays with AAO as template

In order to make CNTs-application products, one of the important milestones is to fabricate CNT arrays. How can we obtain a regular CNTs array at what we

want positions in an efficient way? Surely, we should define and fix the catalyst position, or give them a template. Then use some typical means like CVD to growth CNTs. In the past decade, a lot of methods to locate the position of catalyst or making template had been report. In conclusion, these methods were nothing more than lithography pre-pattern<sup>[Vladimir-2001-1178, Ren-1999-1086]</sup>, chemical pre-pattern<sup>[Dongsheng-1999-481]</sup> or using template. As decribed in section 1.2, lithography is an extreme precise but time-consuming and expensive way. Besides, it still has a limitation about 80nm size. If we want a tinier scale, it still has some problems until now. While AAO can't define such an exact spot like lithography, it remains very useful in some applications which need ordered but not so accurate positions array in large area. This just have the same idea by coincidence with certain applications of CNTs.

AAO assisted growth of CNTs has been done by many research team. To make a comprehensive survey, it can be separate into two main types. One is using AAO with catalyst<sup>[Lee-2001-2387, Jeong-2002-1859]</sup>; the other is use only AAO without any other catalyst.<sup>[Yuan-2001-3127, Takashi-1996-2109]</sup>

According to the reports of these papers, the result of using AAO with catalyst shows in fig. 2-17. From the SEM image [Fig. 2-17(a)], it is very clear that the tube length would hardly control. But in the high resolution TEM (HRTEM) image [Fig. 2-17(b)], the continuous graphene layers can be observed.

And the electron diffraction(ED) pattern inset the [fig. 2-17(b)] shows the rings of graphite. This implies the crystalline of CNTs is good. On the other hand, the AAO without catalyst method always lead to controllable tube length[Fig. 2-18(a)] but the ED pattern showing a disk shape suggests poor crystallinity [Fig. 2-18(b)]. To complete the two respects remains the goals that researchers want to accomplish.

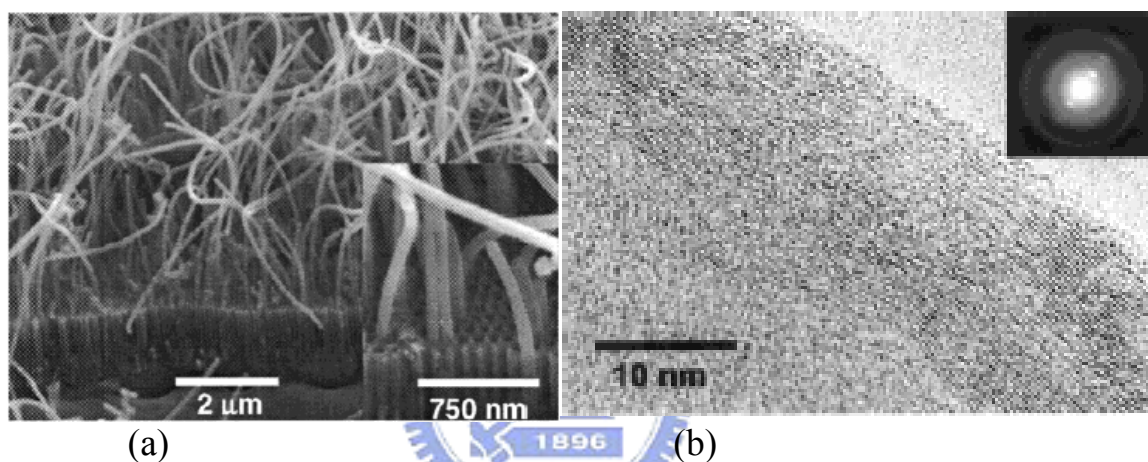


Fig. 2-17. (a)The SEM<sup>[Jeong-2002-1859]</sup> and (b)HRTEM and ED pattern<sup>[Jeong-2002-4003]</sup> of CNTs image of using AAO with catalyst.

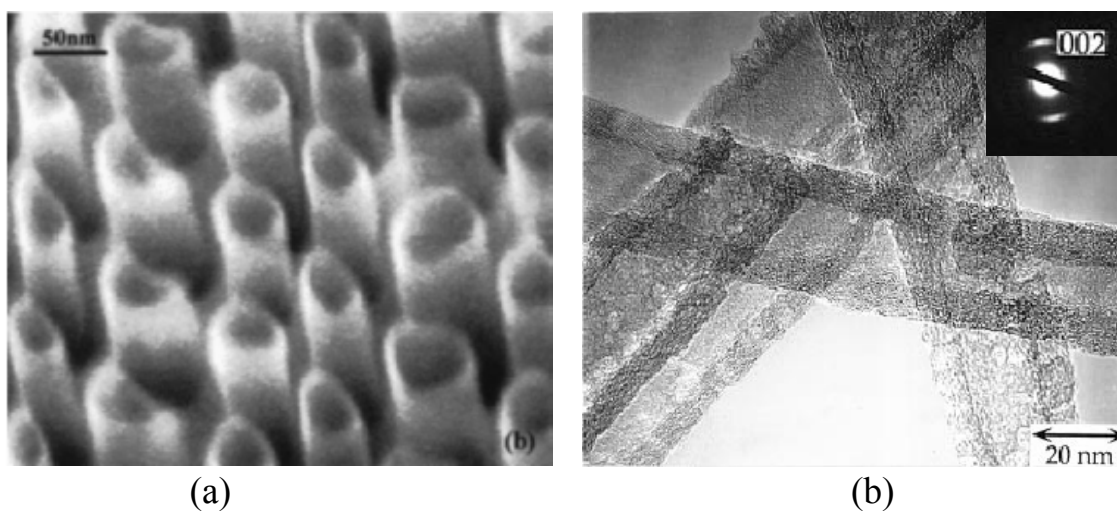


Fig. 2-18. (a)The SEM<sup>[Yuan-2001-3127]</sup> and (b)HRTEM<sup>[Takashi-1996-2109]</sup> with inset ED pattern of using AAO without catalyst

Moreover, another important point in growth CNTs array is density control. In many applications like FED or fuel cell, tube number density directly affect the performance. In 2002, Tu et al. use pulse-current electrochemical deposition method to prepare Ni nanoparticles that are used as the catalysts for the growth of aligned carbon nanotubes.<sup>[Tu-2002-4018]</sup> The nucleation site density of the Ni nanoparticles was controlled by changing the magnitude and duration of the pulse current.<sup>[Michael-2000-878]</sup> The aligned carbon nanotubes from the nickel nanoparticles were grown by plasma enhanced hot filament chemical vapor deposition. The site density of the aligned carbon nanotubes varied from  $10^5$  to  $10^8$  tubes/cm<sup>2</sup> counts on density of Ni nanoparticle. [Figs. 2-19(a)-(e)]

But in growth CNTs use AAO as template, it needs to find another way of controlling density. Jeong et. al controlled the density of tubes from  $10^5$ - $10^9$  tubes/cm<sup>2</sup> order by changing the aspect ratio of AAO nanopores.<sup>[Jeong-2002-4003]</sup> They proceeded the same process condition in two different AAO samples with different aspect ratio taking advantage of the hydrocarbon radical diffusion behavior to control density. They purposed at initial stage of deposition CNTs growth and carbon deposition on the pore wall occurs simultaneously. As the synthesis continues, the deposited carbon on the internal pore surface prevents the liftoff of Co catalysts at the tip of the growing CNTs, resulting in short CNTs inside the pores. However, the CNTs, which have already escaped from the

pores, can continuously grow. Precursor molecules collided mainly with the pore walls so that the effect of pore geometry is amplified; in other words, carbon deposition on the pore walls would be more noticeable in an AAO template of smaller and deeper pores. They also show that the density can be changed by passing through the sonication process after growth of CNTs. [Jeong-2002-1859]

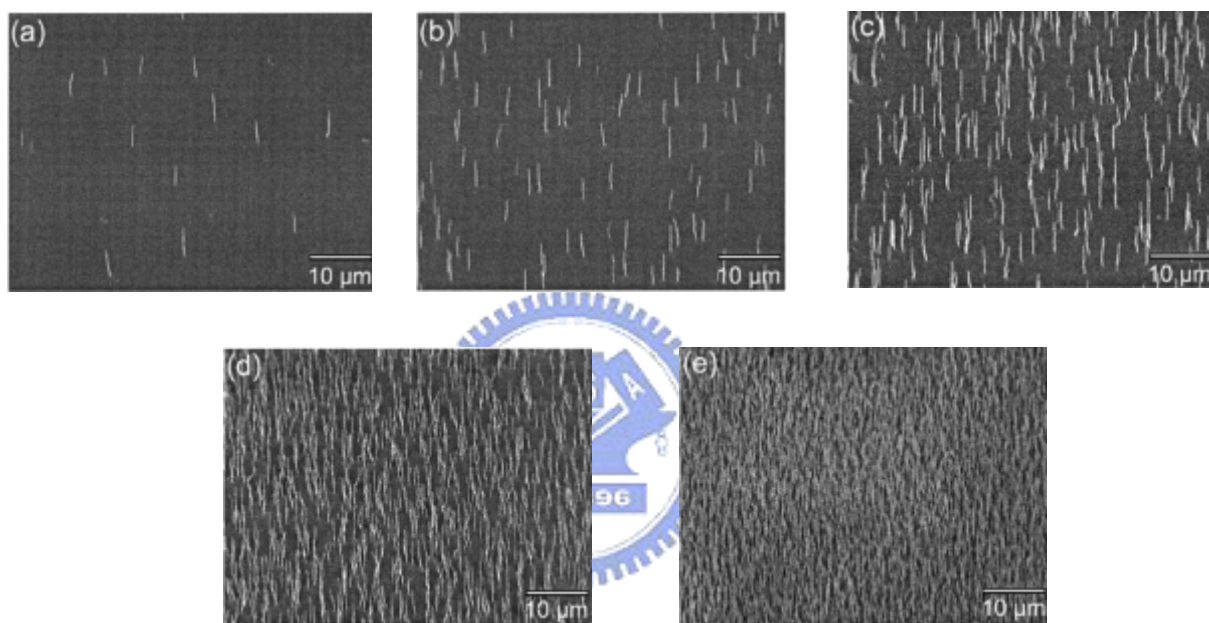


Fig. 2-19. SEM images of aligned CNTs with site density of (a)  $7.5 \times 10^5 \text{ cm}^{-2}$ , (b)  $2 \times 10^6 \text{ cm}^{-2}$ , (c)  $6 \times 10^6 \text{ cm}^{-2}$ , (d)  $2 \times 10^7 \text{ cm}^{-2}$ , (e)  $3 \times 10^8 \text{ cm}^{-2}$ . [Tu-2002-80-4018]